1521-0111/12/8103-356–365$25.00
MOLECULAR PHARMACOLOGY
Copyright © 2012 The American Society for Pharmacology and Experimental Therapeutics
Mol Pharmacol 81:356–365, 2012

Vol. 81, No. 3
75648/3747531

Defining Substrate and Blocker Activity of Alanine-Serine-Cysteine Transporter 2 (ASCT2) Ligands with Novel Serine Analogs

Thomas Albers, William Marsiglia, Taniya Thomas, Armanda Gameiro, and Christof Grewer

Department of Chemistry Binghamton University, Binghamton, New York

Received September 8, 2011; accepted November 23, 2011

ABSTRACT

The neutral amino acid transporter alanine-serine-cysteine transporter 2 (ASCT2) belongs to the solute carrier 1 (SLC1) family of solute transporters and transports small, neutral amino acids across the membrane, including the physiologically important and ubiquitous amino acid glutamine. Our understanding of the involvement of ASCT2 in the physiological processes involving glutamine is hampered by a lack of understanding of its pharmacology and the absence of high-affinity inhibitors. In this study, we combined an in silico docking approach with experimental investigation of binding parameters to develop new ASCT2 inhibitors and substrates, a series of serine esters, and to determine structural parameters that govern their functional effects. The series of compounds was synthesized using standard methods and exhibited a range of properties, from inhibitors to partial substrates and full substrates. Our results suggest that amino acid derivatives with small side-chain volume and low side-chain hydrophobicity interact strongly with the closed-loop form of the binding site, in which re-entrant loop 2, the presumed extracellular gate for the substrate binding site, is closed off. However, these derivatives bind weakly to the open-loop form (external gate open to the extracellular side), acting as transported substrates. In contrast, inhibitors bind preferentially to the open-loop form. An aromatic residue in the side chain is required for high-affinity interaction. One of the compounds, the L-serine ester serine biphenyl-4-carboxylate reversibly inhibits ASCT2 function with an apparent affinity of 30 μM.

Introduction

Glutamine is an important amino acid that is involved in many cellular processes (Neu et al., 1996). Glutamine is shuttled across cellular membranes by a variety of transport systems (Bode, 2001). One of these systems, the neutral amino acid transporter ASCT2, was shown to belong to the solute carrier 1 family of transporters (Utsunomiya-Tate et al., 1996). ASCT2 is specific for transporting small, neutral amino acids, such as glutamine, alanine, serine, and cysteine (Bass et al., 1981; Utsunomiya-Tate et al., 1996). In contrast to ASCT2, the closely related SLC1 family member ASCT1 was shown to lack affinity for glutamine (Arriza et al., 1993). ASCT2 was reported to be an obligate amino acid exchanger (Bröer et al., 2000). Thus, amino acid uptake is strictly coupled to amino acid release (exchange) of an intracellular amino acid. This exchange requires the presence of Na^+, because amino acid translocation is coupled to the cotranslocation of at least one sodium ion (Bröer et al., 2000; Grewer and Grabsch, 2004). In addition to the amino acid exchange function, ASCT2 displays a channel-like anion conductance that depends on the presence of Na^+ and is amplified by binding of transported substrates and inhibited in the presence of competitive inhibitors (Bröer et al., 2000; Grewer and Grabsch, 2004).

ASCT2 is expressed in many tissues, including the brain, in which it may contribute to glutamine homeostasis of neurons and astrocytes (Bröer and Brookes, 2001; Deitmer et al., 2003; Gliddon et al., 2009). It was hypothesized, for example, that ASCT2 mediates efflux of glutamine from astrocytes, a process that is critical for the functioning of the glutamate-glutamine cycle, which recycles synaptically released glutamate. Despite this seemingly important role, the pharmacol-

This work was supported by the National Institutes of Health National Institute of Neurological Disorders and Stroke [Grant 2R01-NS049335-06A1] (to C.G.); and the Binational Science Foundation [Grant 2007051] (to C.G.).
Article, publication date, and citation information can be found at http://molpharm.aspetjournals.org.
http://dx.doi.org/10.1124/mol.111.075648.

ABBREVIATIONS: ASCT, alanine-serine-cysteine transporter; EAAT, excitatory amino acid transporter; HEK, human embryonic kidney; DMSO, dimethyl sulfoxide; NaMes, sodium methanesulfonate; Glt_{Ph}, glutamate transporter homolog from *Pyrococcus horikoshii*; PDB, Protein Data Bank; RL, re-entrant loop; TBOA, DL-threo-β-benzyloxyaspartic acid; LAT, system L-amino acid transporter.

ogy of ASCTs is not well understood. Although the specificity for a large variety of transported substrates has been studied, not much is known about inhibitors of ASCT2 amino acid transport (Grewer and Grabsch, 2004; Esslinger et al., 2005). A few inhibitors have been developed based on homology of the amino acid binding site with the related glutamate transporters from the excitatory amino acid transporter (EAAT) family (Grewer and Grabsch, 2004). In particular, a series of glutamine derivatives was developed with substituents that alter the pK_a value of a proposed hydrogen bond donor in the form of the amide NH bond (Esslinger et al., 2005). However, affinities were in the 500 μM to low millimolar range, and no distinctions were made with regard to the structural properties that differentiate inhibitors from transported substrates.

Here, we aimed at performing structure-function studies to develop inhibitors with higher binding affinity, as well as to obtain a better understanding of the molecular determinants of the compounds that differentiate blockers from transported substrates. We have used a docking approach to identify serine derivatives as potential ligands with a series of substituents attached to the hydroxyl oxygen. Experimental validation of the predicted compounds suggests that the activity of the transported substrates decreases strongly after side-chain volume reaches a threshold. In contrast, inhibitors benefit from hydrophobic bulk in the side chain, in particular when the hydrophobic group is aromatic. The analysis resulted in the development of a blocker with approximately 3-fold higher affinity than the best compounds that have been reported previously.

Materials and Methods

Cell Culture and Transfection

cDNA coding for the rat ASCT2 was kindly provided by S. Bröer (Physiologisches Institut der Universität, Tübingen, Germany) (Bröer et al., 1999; Bröer et al., 2000). The coding region of the cDNA was subcloned into the EcoRI site of the pBK-CMV vector (Stratagene, La Jolla, CA). The cDNA construct was used to transiently transfect subconfluent human embryonic kidney (HEK) 293 cells (American Type Culture Collection, Manassas, VA) with FuGENE HD reagent (Roche Applied Science, Indianapolis), according to the instructions of the supplier. Electrophysiological recordings were performed between days 1 and 2 after transfection.

Electrophysiological Techniques

ASCT2-mediated currents were recorded with an Adams and List EPC7 amplifier (HEKA, Lambrecht, Germany) under voltage-clamp conditions. The whole-cell current-recording configuration was used (Hamill et al., 1981). Electrode resistances were 2 to 3 MΩ, and the series resistance (R_S) was 5 to 8 MΩ. Series resistance was not compensated, because compensation had no effect on the magnitude of the observed currents. The extracellular bath solution contained 140 mM sodium methanesulfonate (NaMes) or sodium thiocyanate, 2 mM $Mg(GlcA)_2$, 2 mM $Ca(GlcA)_2$, and 10 mM HEPES, pH adjusted to 7.4 with NaOH. The pipette solution contained 130 mM sodium thiocyanate, 2 mM $MgCl_2$, 10 mM EGTA, 10 mM HEPES, and 10 mM L-alanine (pH adjusted to 7.3 with NaOH). Using this intracellular solution, the transporters are operated in the exchange mode, in which external alanine is exchanged with internal alanine in the absence of net transport. The exchange mode is associated with the activation of an uncoupled anion current, which was used as an assay for ASCT2 function. The currents were low-pass filtered at 3 kHz (EPC7 built-in filter) and digitized with a digitizer board (Digidata 1200; Molecular Devices, Sunnyvale, CA) at a sampling rate of 10 to 50 kHz (controlled by software, pClamp7). All experiments were performed at room temperature.

Rapid solution exchange was essentially performed as described previously (Grewer et al., 2000; Watzke et al., 2001). In brief, substrates and inhibitors were applied to the ASCT2-expressing HEK293 cells with a quartz tube (350-μm tube diameter) positioned at a distance of $\approx$ 0.5 mm to the cell. The linear flow rate of the solutions emerging from the opening of the tube was approximately 5 to 10 cm/s, resulting in typical rise times of the whole-cell current of 30 to 50 ms (10–90%).

Data Analysis

Nonlinear regression fits of experimental data were performed with Origin (OriginLab Corp, Northampton, MA) or Clampfit (pClamp8 software; Molecular Devices). Dose-response relationships of currents were fitted with a Michaelis-Menten-like equation, yielding K_m and I_{max}. Each experiment was performed in triplicate with at least two different cells. The error bars represent mean $\pm$ S.D. unless stated otherwise.

Docking Procedure

Homology models were built using two structures of the Glt_{Ph} as templates: that is PDB ID 2NWX [aspartate-bound, reentrant loop RL2 closed (Boudker et al., 2007)] and PDB ID 2NWW [inhibitor-bound, reentrant loop RL2 open]. Alignments were generated using ClustalW or HHPred (Söding et al., 2005) with similar results because of the high sequence similarity (85%) in the substrate binding region. Outputs of the pair-wise sequence alignments were used to create structural homology models with the Modeler software (Eswar et al., 2007). For Protein Data Bank ID 2NWX as the template, Modeller was programmed to include the two bound cations in the homology model. The resulting structure files were tested for quality with the ProQ program (Wallner and Elofsson, 2003) to test for correct helical assignment of the transmembrane segments.

Docking was performed using the Autodock Vina program (Trott and Olson, 2010), using PyRx as the front-end for ligand preparation and positioning of the binding box (Wolf, 2009). Ligands were initially generated using ChemSketch (Advanced Chemistry Development, Inc., Toronto, ON, Canada), setting the correct protonation states for pH 7.3 using Open Babel (http://openbabel.sourceforge.net/). Subsequently, ligands were imported into PyRx and energy-minimized using the UFF force field. The box for docking was set as cubic, 15-Å wide, and centered at the C_β atom of the bound amino acid molecule.

Synthesis

All chemicals were purchased from VWR. The compounds were prepared according to the following procedures.

(*S*)-3-(*tert*-Butoxy)-2-((*tert*-butoxycarbonyl)amino)-3-oxopropyl cyclohexanecarboxylate (1b). In a round-bottomed flask, *N*-butyloxycarbonyl serine *tert*-butyl ester (0.2 g, 0.765 mmol) was dissolved in dichloromethane. Cyclohexanecarbonyl chloride **(1a)** was then added along with 4-dimethylaminopyridine (9.3 mg, 0.0765 mmol) and triethylamine (0.133 ml, 0.956 mmol). The reaction was stirred overnight. The next day, the mixture was evaporated of dichloromethane, extracted once with ice-cold 2 M hydrochloric acid, and extracted twice with sodium bicarbonate and once with brine. The organic layer was dried by passing it through a glass Büchner funnel filled with magnesium sulfate. The material was purified by column chromatography using ethyl acetate/dichloromethane (1:20). ^{1}H NMR (300 MHz, $CDCl_3$): 5.3 (s, 1H), 4.45 (d, 2H), 2.53 (m, 1H), 1.92 to 1.11 (m, 5H), 1.44 (s, 18H).

(*S*)-*tert*-Butyl-3-(2-(9*H*-fluoren-3-yl)acetoxy)-2-((*tert*-butoxycarbonyl)amino)propanoate (2b). The serine ester (**2b**) was made using 175 mg (0.765mmol) of 9*H*-fluorene-2-carbonyl chloride (**2a**). Purification of the serine ester was done by column chromatography using the solvent system dichloromethane/ethyl acetate (10:1). ^{1}H NMR (300 MHz, $CDCl_3$): 8.21 (s, 1H), 8.05 (d, 1H), 7.85 (t, 2H), 7.57 (d, 1H), 7.45 (m, 2H), 4.45 (d, 1H), 4.67 to 4.51 (m, 3H), 3.95 (s, 2H), 1.51 (s, 18H). **2c**:

^{1}H NMR (300 MHz, DMSO-d_6): 8.95 to 8.56 (s, 3H), 8.37 (s, 1H), 8.35 to 8.05 (m, 3H), 7.82 to 7.65 (m, 1H), 7.64 to 7.43 (m, 2H), 4.85 to 4.55 (m, 3H), 4.23 to 4.07 (s, 2H).

(*S*)-3-(*tert*-Butoxy)-2-((*tert*-butoxycarbonyl)amino)-3-oxopropyl-2-naphthoate (3b). The serine ester (**3b**) was made using 146 mg (0.765 mmol) of 2-naphthoyl chloride (**3a**). Purification by column chromatography was done using a solvent system of dichloromethane/ethyl acetate (19:1). ^{1}H NMR (300 MHz, $CDCl_3$): 8.55 (s, 1H), 8.05 to 7.81 (m, 4H), 7.55 (m, 2), 5.42 (d, 1H), 4.72 to 4.56 (m, 3H), 1.45 (s, 18H). **3c**: ^{1}H NMR (300MHz, DMSO-d_6): 8.91 to 8.62 (s, 3H), 8.23 to 8.03 (m, 5H), 7.85 to 7.71 (m, 2H), 4.89 to 4.55 (m, 3H).

(*S*)-*tert*-Butyl-2-(*tert*-butoxycarbonyl)amino)-3-(isobutyryloxy)propanoate (4b). The serine ester (**4b**) was prepared in the same manner, using 67 mg of isobutyryl chloride (0.765 mmol) (**4a**). The oil was purified using column chromatography using the solvent system dichloromethane/ethyl acetate (1:1). ^{1}H NMR (300 MHz, $CDCl_3$): 5.27 (d, 1H), 4.49 to 4.15 (m, 3H), 2.53 (septet, 1H), 1.45 (s, 18H), 1.16 (d, 6H).

(*S*)-3-(*tert*-Butoxy)-2-((*tert*-butoxycarbonyl)amino)-3-oxopropyl[1,1′-biphenyl]-4-carboxylate (5b). The serine ester was also prepared in the same way as (**3b**), using 0.17 g of [1,1′-biphenyl]-4-carbonyl chloride (0.765 mmol) (**5a**). The solvent system used for column chromatography was dichloromethane/ethyl acetate (7:3). ^{1}H NMR (300 MHz, $CDCl_3$): 8.42 to 7.40 (m, 9H), 5.51 to 5.48 (s, 1H), 4.72 to 4.52 (m, 2H), 3.97 to 3.83 (m, 1H), and 1.68 to 1.39 (s, 18H).

(*S*)-*tert*-Butyl-2-(*tert*-butoxycarbonyl)amino)-3-(propionyloxy)propanoate (6b). To a solution of propionic acid (51.45 mg, 0.695 mmol) dissolved in dichloromethane was added *tert*-butyl 2-((*tert*-butoxycarbonyl)amino)-3-hydroxypropanoate (0.2 g, 0.765 mmol), *N*,*N*′-dicyclohexylcarbodiimide (0.16 g, 0.765 mmol), and 4-dimethylaminopyridine (8.5 mg, 0.0695 mmol). The mixture was magnetically stirred overnight in a round-bottomed flask. The reaction mixture was filtered of *N*,*N*′-dicyclohexyl urea, and the filtrate was extracted thrice with water, thrice with 5% citric acid in water, and thrice with water. The organic layer was diluted with dichloromethane and was then magnetically stirred overnight in an Erlenmeyer flask with magnesium sulfate to remove traces of water. The organic layer was then filtered and evaporated. The resulting yellow oil was purified using column chromatography. The solvent system used was dichloromethane/ethyl acetate (1:10). ^{1}H NMR (300 MHz, $CDCl_3$): 5.28 (d, 1H), 4.45 (d, 2H), 4.25 (m, 1H), 2.34 (q, 2H), 1.45 (s, 18H), 1.11 (t, 3H).

(*S*)-1-Carboxy-2-((cyclohexanecarbonyl)oxy)ethanaminium) tris(2,2,2-trifluoroacetate) (1c). A mixture of dichloromethane/trifluoroacetic acid (1:10) was added to a flask containing **1b**. The mixture was magnetically stirred for 3 h and was then evaporated of trifluoroacetic acid and dichloromethane to produce the deprotected product **3**. ^{1}H NMR (360 MHz, DMSO-d_6): 8.51 (s, 3H), 4.42 (m, 2H), 4.15 (m,1H), 2.55 to 1.15 (m, 5H).

The rest of the compounds (**2c**–**6c**) were deprotected in the same manner as **1c**:

Mono((*S*)-2-(((9*H*-fluorene-2-carbonyl)oxy)-1-carboxyethanaminium) tris(2,2,2-trifluoroacetate) (**2c**) ^{1}H NMR (300 MHz, DMSO-d_6): 8.85 to 8.45 (*s*, 3H), 8.35 to 7.31 (m, 7H), 4.85 to 4.47 (m, 3H), 4.23 to 3.91 (s, 2H)

(*S*)-2-(((2-naphthoyl)oxy)-1-carboxyethanaminium)tris(2,2,2-trifluoroacetate) (**3c**) ^{1}H NMR (300 MHz, DMSO-d_6): 8.83 to 8.54 (3H), 8.21 to 7.64 (m, 7H), 4.82 to 4.51 (m, 3H),

(*S*)-1-carboxy-2-((isobutyryloxy)ethanaminium)tris(2,2,2-trifluoroacetate) (**4c**) ^{1}H NMR (300 MHz, DMSO-d_6): 8.62 to 8.43 (s,3H), 4.35 (m, 3H), 2.56 (septet, 1H), 1.12 (s, 6H),

(*S*)-2-((([1,1′-biphenyl]-4-carbonyl)oxy)-1-carboxyethanaminium) tris(2,2,2-trifluoroacetate) (**5c**) ^{1}H NMR (300 MHz, DMSO-d_6): 8.81 to 8.62 (s, 3H), 8.21 to 7.33 (m, 9H), 4.83 to 4.68 (m, 2H), 4.62 to 4.50 (m, 1H),

(*S*)-1-carboxy-2-((propionyloxy)ethanaminium)tris(2,2,2-trifluoroacetate) (**6c**) ^{1}H NMR (300 MHz, DMSO-d_6): 8.53 to 8.45 (s, 3H), 4.63 to 4.27 (m, 3H), 2.41 to 2.29 (q, 2H), 1.10 to 0.99 (t, 3H).

Results

In Silico Docking Studies Predict Open-Loop or Closed-Loop Preference of Substrates and Inhibitors. In an effort to predict the structure of ligands that interact with the ASCT2 amino acid binding site with reasonable affinity, we used a ligand-docking approach. The docking templates were homology models of ASCT2 based on the crystal structures of an homologous archaeal aspartate transporter, Glt_{Ph} (Yernool et al., 2004; Boudker et al., 2007). Although the overall identity between the ASCT2 and Glt_{Ph} sequences is low (30% identity, 50% similarity), the amino acid binding site (residues in 4-Å distance of the bound ligand) is very well conserved with 69% identity and 85% similarity. In fact, only two side chains that contribute to the ligand binding site are not conserved, which are Cys479 (corresponding to Arg397 in Glt_{Ph}) and Ala402 (corresponding to Thr314 in Glt_{Ph}). The Arg-to-Cys substitution in transmembrane domain 8 is known to be mainly responsible for the different substrate selectivities of the two transporters (Bendahan et al., 2000). In Glt_{Ph}, the positively charged side chain of Arg397 forms a salt bridge with the β-carboxylate of aspartate (Yernool et al., 2004). This electrostatic interaction is absent in the ASCTs, accounting for their propensity to bind neutral amino acid substrates.

To test the docking approach, we first performed control docking studies using the known, aspartate-bound crystal structure of Glt_{Ph} as the template [PDB ID 2NWX (Boudker et al., 2007)]. Docking was performed in Autodock Vina, using a 15-Å cubic box centered at the C_β atom of the bound aspartate molecule. Five poses were found by the docking algorithm, but only one of these poses (pose 0 with the lowest binding free energy; Table 1) displayed the correct orientation of the α NH_3^+ and COO^- groups. This pose is shown in Fig. 1A, superimposed with the native aspartate ligand from the crystal structure (root-mean-square deviation = 0.73). The slight difference in predicted and experimental pose is caused by a slightly altered position of the β-carboxylate (Fig. 1A), whereas the binding positions of the α NH_3^+ and COO^- groups are well preserved. Overall, this analysis suggests that the docking procedure is capable of detecting physically relevant conformations of bound ligands in EAAT proteins.

We then used the docking approach to predict the interaction of neutral amino acid derivatives with ASCT2. We used two separate homology models based on templates 2NWX, [termed ASCT2(2NWX)] and 2NWW [termed ASCT2(2NWW)] (Boudker et al., 2007). The former represents the substrate-bound conformation (closed re-entrant loop, RL2; termed *closed-loop form*), whereas the latter was proposed to be more representative of the substrate-free, apo state of the transporter [open RL2, termed *open-loop form* (Boudker et al., 2007; Huang and Tajkhorshid, 2008)]. L-Asparagine is a well characterized transported substrate, which was used first due to its high homology to the aspartate molecule bound to the Glt_{Ph} template. Only poses with the native orientation of the α NH_3^+ and COO^- groups were evaluated [one of nine for Asn, closed RL2, ASCT2(2NWX); Table 1]. This pose is shown in Fig. 1B, superimposed over the aspartate molecule bound to the Glt_{Ph} template, and a docked serine ligand. In contrast to the closed-loop conformation, asparagine is predicted to interact less strongly with the open-loop configuration [two of five poses, open RL2, ASCT2(2NWW); Table 1], which in Glt_{Ph} is known to be the inhibitor-bound form [ligand is DL-threo-β-benzyl-

TABLE 1
Parameters for ASCT2 substrates and inhibitors obtained by docking using Autodock Vina

	ASCT2 Homology Model						ΔG(2NWX)/ ΔG(2NWW)
	Based on 2NWX			Based on 2NWW			
	No. of Evaluated Poses	No. of Poses with Native α-NH_2, COOH	ΔG	No. of Evaluated Poses	No. of Poses with Native α-NH_2, COOH	ΔG	
			kcal/mol			*kcal/mol*	
Serine	9	1	−4.3 (pose 4)	5	2	−3.7 (pose 1)	1.16
Asparagine	9	1	−4.5 (pose 8)	5	2	−4.1 (pose 3)	1.10
Glutamine	9	1	−5.4 (pose 2)	5	2	−4.4 (pose 3)	1.23
-Ethyl (**6c**)	5	1	−5.8 (pose 0)	5	4	−4.7 (pose 0)	1.23
-Isopropyl (**4c**)	5	1	−5.7 (pose 2)	8	2	−4.3 (pose 5)	1.33
-Cyclohexyl (**1c**)	9	1	−3.8 (pose 0)	9	4	−5.3 (pose 1)	0.72
-Bzl-Ser	9	2	−4.6 (pose 0)	7	4	−5.2 (pose 1)	0.88
-Naphthyl (**3c**)	5	0		7	3	−6.1 (pose 5)	
-Biphenyl (**5c**)	9	0		9	2	−6.6 (pose 6)	
-Fluorenyl (**2c**)	6	0		8	2	−6.4 (pose 5)	
Aspartate transporter Aspartate	5	1	−5.5 (pose 0)	5	1	−4.3 (pose 2)	1.28

oxyaspartic acid (TBOA)]. Similar effects were observed with the native substrates L-glutamine and L-serine (Table 1), glutamine being predicted to bind an order of magnitude more strongly to the closed- than to the open-loop form.

To test the effect of alterations to the amino acid substrate side chain on docking behavior, we generated serine derivatives with different substituents, linked to the serine hydroxyl with an ester linkage (the structures of the new compounds are illustrated in Fig. 2, together with those of some common amino acid substrates). The ethyl (**6c**), isopropyl (**4c**), and cyclohexyl (**1c**) derivatives could be modeled into the ligand binding site of the closed-loop structure by Autodock Vina. It should be noted that the cyclohexyl (**1c**) derivative model scored low for binding affinity ($\Delta G = -3.8$ kcal/mol; Table 1). Serine derivatives with larger, aromatic substituents [naphthyl (**3c**) and fluorenyl (**2c**)] were excluded from the binding site in the closed-loop form (Table 1), based on the size of the substituent. In contrast, the naphthyl and fluorenyl derivative models scored high for binding to the open-loop form, whereas the compounds with isopropyl substituent and smaller side chains received a low score in this binding configuration (Table 1). One of the poses for benzylserine binding to the open-loop form (pose two of four poses with correct α NH_3^+ and COO^- group orientation) is shown in Fig. 3, A and B, superimposed over the TBOA-bound Glt_{Ph} structure, 2NWW (Boudker et al., 2007). It is evident that the aromatic group adopts a slightly different orientation in benzylserine compared with TBOA, possibly because of the lack of salt-bridge interaction from the missing β-carboxylate.

As will be discussed in the next section, our experimental results demonstrate that compounds scoring high for binding to the closed-loop form, but scoring low for binding to the open-loop form are substrates, whereas compounds with the opposite preference for open-loop rather than closed-loop binding are inhibitors. To quantify this substrate/inhibitor preference, the ΔG(2NWX model)/ΔG(2NWW model) ratio is listed in Table 1 (last column). Compounds with a ratio below 1 are predicted to be inhibitors, whereas those with a ratio >1 are predicted to be substrates.

Experimental Analysis of the Docking Results. Our next aim was to synthesize the compounds predicted from the docking studies and analyze their biological activity. Synthesis was performed according to standard procedures by condensing α NH_2 and COOH protected serine with the substituent carboxylic acid using either the dicyclohexylcarbodiimide method (Sheehan et al., 1956) or the acid chloride (Fig. 2), followed by deprotection of the amino acid. The compounds were tested for their ability to either activate anion current or inhibit leak anion current in ASCT2 heterologously expressed in HEK293 cells. It was previously shown that the transporter-mediated anion current can be used as a measure of transport activity (Bröer et al., 2000; Grewer and Grabsch, 2004). This fact is also well established for the homologous glutamate transporters (Watzke and Grewer, 2001), which have a much more rigorously determined pharmacology (Shimamoto et al., 1998; Bridges et al., 1999; Dunlop et al., 2003; Bridges and Esslinger, 2005; Dunlop and Butera, 2006; Luethi et al., 2010). Transport current cannot be used as an assay for the function of ASCT2 substrates/inhibitors, because ASCT2 is an amino acid exchanger, and thus no steady-state transport current can be observed (Zerangue and Kavanaugh, 1996; Bröer et al., 2000). However, our results demonstrate that inhibitors block charge movement that is induced by voltage-dependent movement of transported substrates across the membrane (not shown), suggesting that the anion current assay reflects on exchange activity.

Transported substrates are known to induce anion current when applied to ASCT2 (Bröer et al., 2000; Grewer and Grabsch, 2004), as shown in Fig. 4A for L-alanine. Although acetyl serine ester (**6c**) was a full substrate, eliciting anion current of the same magnitude as that of alanine, the isobu-

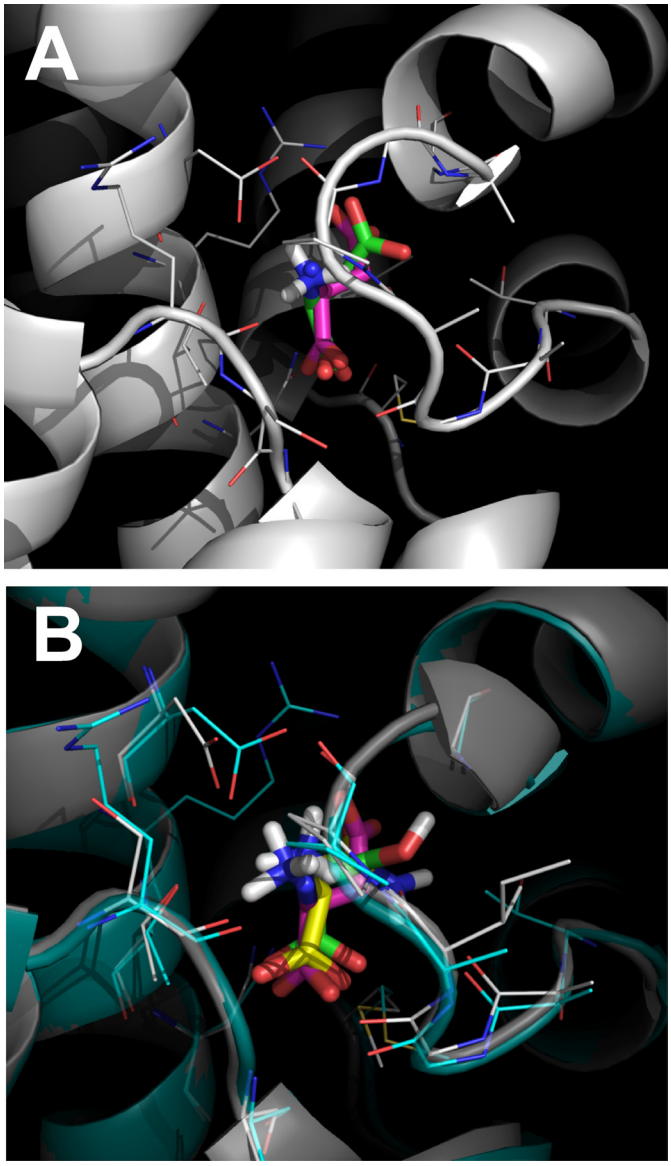

Fig. 1. A, superposition of the native aspartate ligand from the Glt_{Ph} 2NWX structure (pink ligand) with the L-Asp complex predicted by Autodock Vina (based on 2NWX, green ligand). B, superposition of the L-Ser (green) and L-Asn (yellow) ligands docked to the ASCT2(2NWX) homology model (gray structure). The GltPh2NWX structure with the bound ligand; Asp (pink), is shown in turquoise. The amino acid side chains in a distance of 4 Å from the ligands are highlighted as lines.

tyryl ester (**4c**) with the larger substituent volume and increased hydrophobicity was a partial substrate with 26 ± 10% of the maximal alanine-induced current (at saturating concentration; Fig. 4B; Table 2). The kinetic properties of the activating substrates, including their apparent K_m values estimated from dose response curves (Fig. 4B), are listed in Table 2. No measurable anion currents were induced by application of serine cyclohexane carboxylate (**1c**) to ASCT2 (up to 5 mM), indicating that this compound either does not bind to ASCT2 at the tested concentrations or that it binds but is not an activating substrate. The former possibility is more likely, because **1c** at a concentration up to 2 mM was unable to inhibit alanine-induced inward anion currents mediated by ASCT2 alanine exchange (data not shown).

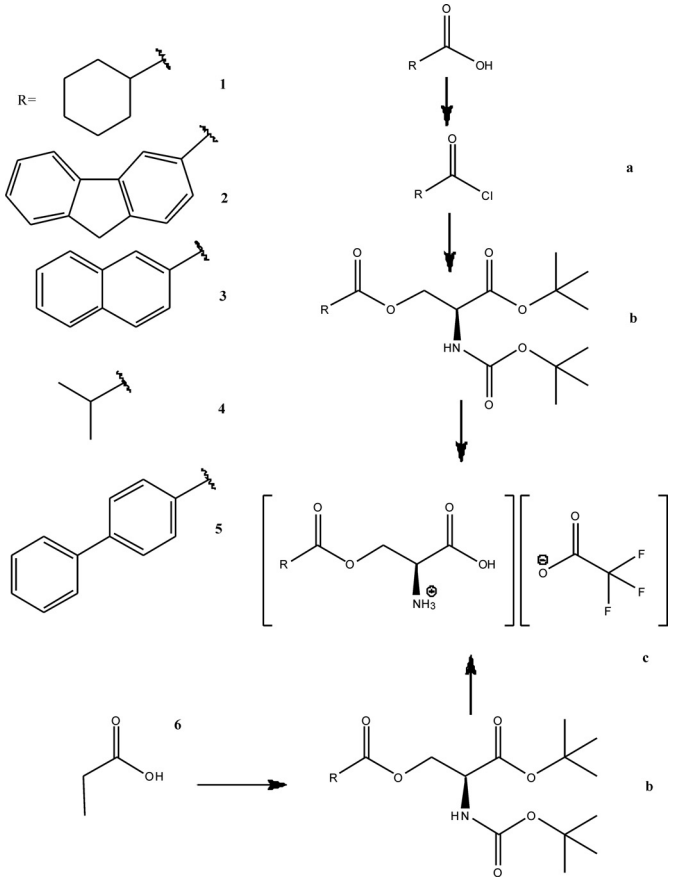

Fig. 2. Summary of structures of amino acid substrates and inhibitors used in this study, and a summary of the synthetic procedures.

Next, we tested compounds that were predicted to be inhibitors from the docking studies. In contrast to transported substrates, inhibitor application mediated an apparent outward current in ASCT2-expressing HEK293 cells (representative original traces shown in Fig. 5A). This outward current was previously shown to be caused by inhibition of a leak inward anion current (Grewer and Grabsch, 2004), in agreement with results obtained for inhibition of the homologous glutamate transporters (EAATs) by the competitive inhibitor TBOA (Grewer et al., 2000, 2005). The apparent outward current was dose-dependent and could be analyzed using a Michaelis-Menten-type equation (Fig. 5B), yielding K_m values listed in Table 2. The maximum currents induced by the inhibitors at saturating concentrations (I_{max} values) were −25 to 30% of those of the maximum alanine-induced current, indicating that the leak anion conductance of ASCT2 carries approximately 30% of the current of the substrate-induced anion conductance, in agreement with previous results obtained for benzylserine (Grewer and Grabsch, 2004). The inhibitor with the highest apparent affinity was biphenyl serine ester (**5c**), with a K_m of 30 ± 6 μM. This affinity is significantly higher than any previously known ASCT2 inhibitor (Grewer and Grabsch, 2004; Esslinger et al., 2005).

To test whether the inhibitors not only block leak anion current, but also inhibit activity of transported substrates, we applied the compounds in the presence of alanine (200 μM). As shown in the representative results in Fig. 5, C to E, **3c** fully inhibited the alanine-induced response and generated leak current block even in the presence of activating

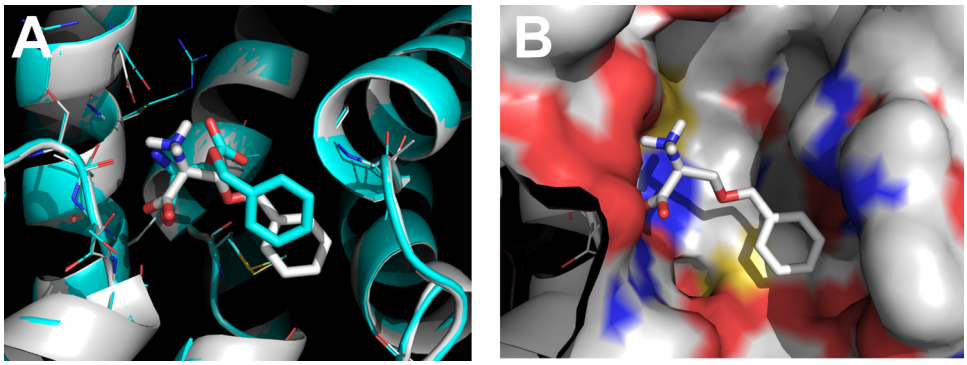

Fig. 3. A, superposition of the native TBOA ligand from the Glt_{Ph} 2NWW structure (turquois ligand) with the L-Bzl-Ser complex (pose 5) predicted by Autodock Vina (based on 2NWW homology model, gray ligand). B, surface representation of the predicted inhibitor binding site.

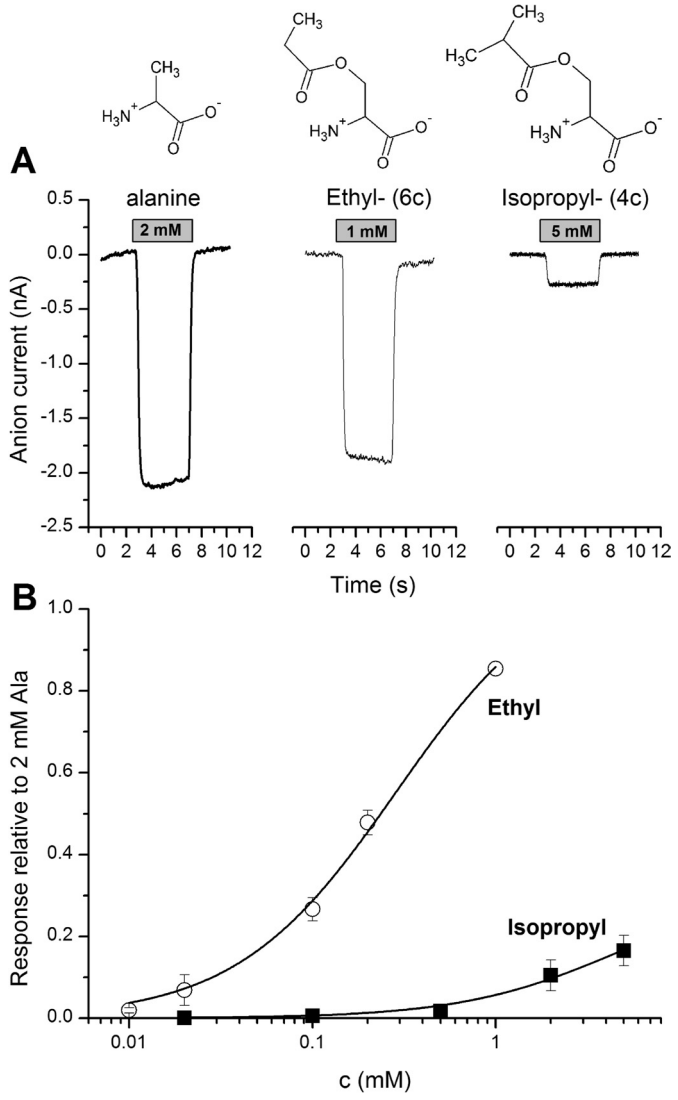

Fig. 4. A, original traces of inward anion currents elicited by the application of full and partial substrates to ASCT2 at the timing and concentration indicated by the gray bar. The baseline current was subtracted. The membrane potential was 0 mV, and the intracellular solution contained 10 mM alanine and 135 mM NaSCN. The extracellular solution contained 140 mM NaMes. B, dose response curves for two of the substrates (■, **4c**, isopropyl-; ○, **6c**, ethyl-). The solid lines represent fits according to the Michaelis-Menten equation.

substrate (Fig. 5C). Compound **5c** was evaluated in more detail, as shown in Fig. 5, D and E. The apparent K_I increased with increasing alanine concentration, as expected

TABLE 2

Kinetic properties of ASCT2 substrates and inhibitors

All values are listed for V_m = 0 mV. Currents are listed relative to the anion current induced by saturating alanine concentration.

	K_m	Relative Current
	μM	
L-Alanine	40 ± 6	1.00
L-Glutamine	25 ± 1	0.98 ± 0.04
-Ethyl (**6c**)	280 ± 30	1.1 ± 0.06
-Isopropyl (**4c**)	4700 ± 500	0.26 ± 0.1
-Cyclohexyl (**1c**)	N.D.	0
-Bzl-Ser	900 ± 400	−0.27 ± 0.1
-Naphtyl (**3c**)	107 ± 29	−0.22 ± 0.03
-Biphenyl (**5c**)	30 ± 6	−0.43 ± 0.07
-Fluorenyl (**2c**)	40 ± 12	−0.29 ± 0.04

N.D., not determined.

for a competitive mechanism. The K_I-versus-alanine concentration relationship calculated according to eq. 1

$$K_I(S) = K_I(0) + [S]\frac{K_I(0)}{K_m(\text{alanine})} \quad (1)$$

fits well to the experimental data, indicating a competitive inhibition mechanism. In this equation, [S] is the concentration of the substrate (alanine), and $K_I(0)$ is the inhibition constant for serine biphenyl-4-carboxylate in the absence of alanine.

$$\frac{I_{inh+ala}}{I_{max}} = \left(\frac{I_{max} - I_{ala}}{I_{max}}\right)\frac{[I]}{[I] + K_I} + \frac{I_{ala}}{I_{max}} \quad (2)$$

In this equation I_{max} represents the current for inhibitor alone, in the absence of alanine, and K_I is the inhibition constant for the inhibitor in the presence of alanine.

Inhibitor Dissociation Kinetics. We used a rapid solution exchange protocol to determine the dissociation of the naphthyl ester, **3c**. The strategy was to pre-equilibrate the cell with the inhibitor, followed by a rapid step into a solution containing a saturating concentration of alanine (Fig. 6, see bars at the top as an illustration of the solution exchange protocol). If the inhibitor needs to dissociate from the binding site before alanine can bind and elicit anion current, then current activation should be slowed compared with activation by alanine in the absence of the inhibitor. Consistent with this expectation, pre-exposure of ASCT2 to **3c** leads to an approximately 2-fold increase in the activation time constant (Fig. 6, A and B). It should be noted that the time resolution of our solution exchange device is in the 5- to 8-ms range, as tested by recording open pipette tip currents upon changing solutions with varying salt concentrations. Therefore, the activation time constant in the absence of the inhibitor is limited by the time resolution of the solution exchange

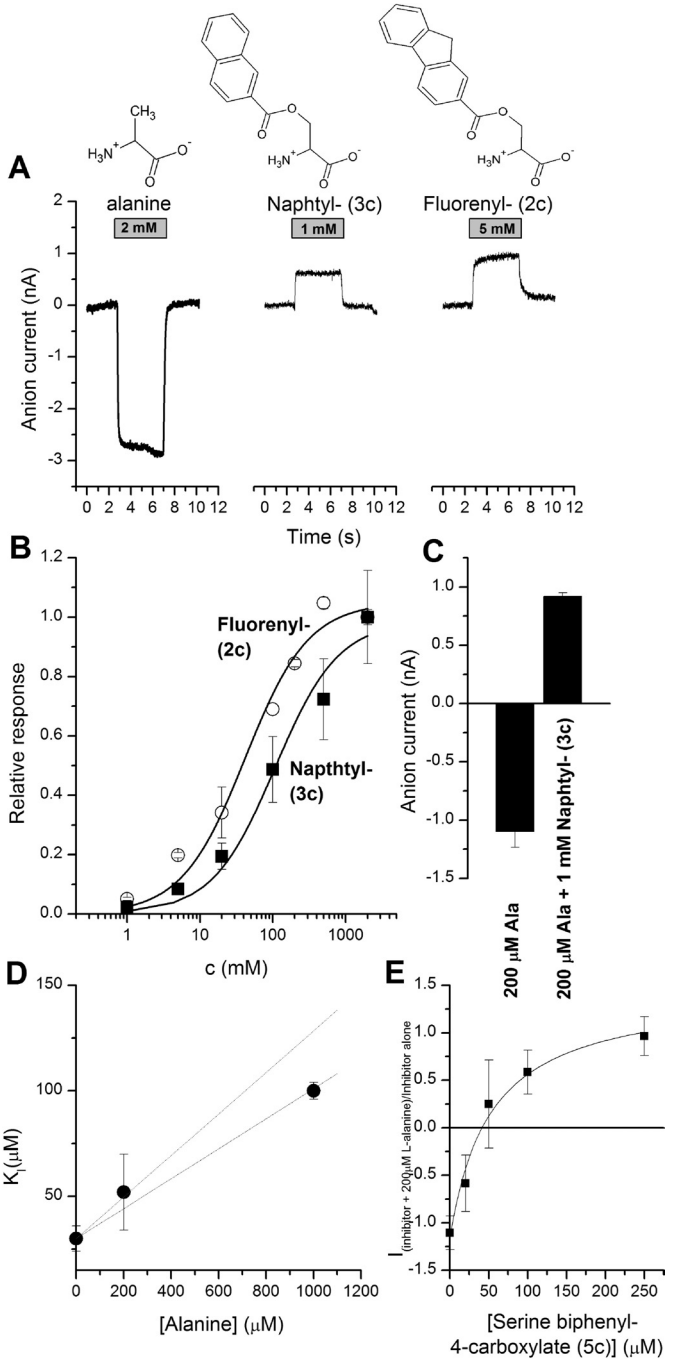

Fig. 5. A, original traces of inward anion currents elicited by the application of alanine (left trace) and inhibited leak anion current by the application of inhibitors to ASCT2 at the timing and concentration indicted by the gray bar. The baseline current was subtracted. The membrane potential was 0 mV and the intracellular solution contained 10 mM alanine and 135 mM NaSCN. The extracellular solution contained 140 mM NaMes. B, dose response curves for two of the inhibitors (**2c** and **3c**). The solid lines represent fits according to the Michaelis-Menten equation. C, **3c** inhibits the current response to 200 μM alanine (ionic conditions as in A). D, inhibition constant, K_I, for serine biphenyl-4-carboxylate (**5c**) at different concentrations of alanine. The dashed lines show the relationship expected for competitive inhibition, according to eq. 1. The fact that two lines are shown reflects the error in the K_m determined for alanine. E, for inhibition of the currents in the presence of both inhibitor (**5c**) and alanine (shown here for 200 μM alanine), eq. 2 was used to fit the data.

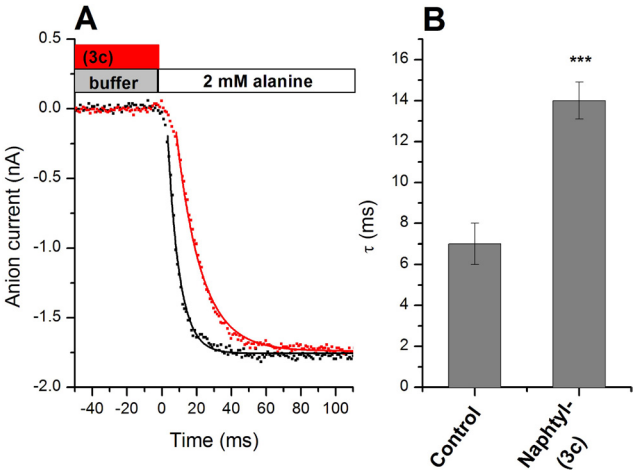

Fig. 6. Inhibitor dissociation kinetics. A, rapid solution exchange from a solution containing only extracellular buffer (control, black dots) to a solution containing buffer + 2 mM alanine, as indicated by the bars (top). The red dots show an analogous experiment, in which the cell was preincubated with 1 mM **3c**. Subsequent application of alanine leads to the displacement of **3c**, allowing the determination of dissociation kinetics. The baseline current was subtracted. The membrane potential was 0 mV and the intracellular solution contained 10 mM alanine and 135 mM NaSCN. The extracellular solution contained 140 mM NaMes. B, quantification of time constants from the exponential fits shown as solid lines in A. Note that the time constant for the alanine activation of the current is limited by the time constant of the solution exchange.

device. Assuming that the slower kinetics of the inhibitor displacement experiment are not limited by solution exchange kinetics, a dissociation constant of **3c** from its binding site of 72 s^{-1} can be estimated.

Structure-Activity Analysis of ASCT2 Substrates and Inhibitors. Previous work on the homologous acidic amino acid transporters (EAATs) showed that bulk of the bound amino acid side chain is an important determinant for the strength of interaction of the ligand with its binding site, as well as for defining substrate or inhibitor properties. To test whether ASCT2 ligand behavior obeys similar principles, we analyzed the apparent affinity of the interaction with the protein as a function of amino acid properties, such as side-chain volume and hydrophobicity, as defined by log(P) (Fig. 7). The data suggest that the affinity of activating substrates increases with decreasing side-chain volume as well as side-chain hydrophobicity. In contrast, the affinity of inhibitors increases with increasing side-chain volume and log(P) (Fig. 7).

Next, we extended the structure-activity analysis to the ability of the compounds to induce or inhibit anion current. As shown in Fig. 8, compounds with a side-chain volume below 110 $Å^3$ are activating substrates, whereas compounds with higher side chain volume are either inactive (i.e., do not bind, such as **3c**), or inhibit the leak anion conductance. This result suggests the existence of a size-exclusion limit for the binding of activating substrates to their ASCT2 binding site, as predicted by the docking analysis.

Discussion

Here, we combined in silico docking with a functional assay to gain insight into the mechanisms that govern substrate recognition by the neutral amino acid transporter ASCT2. The docking analysis led to a congeneric series of compounds

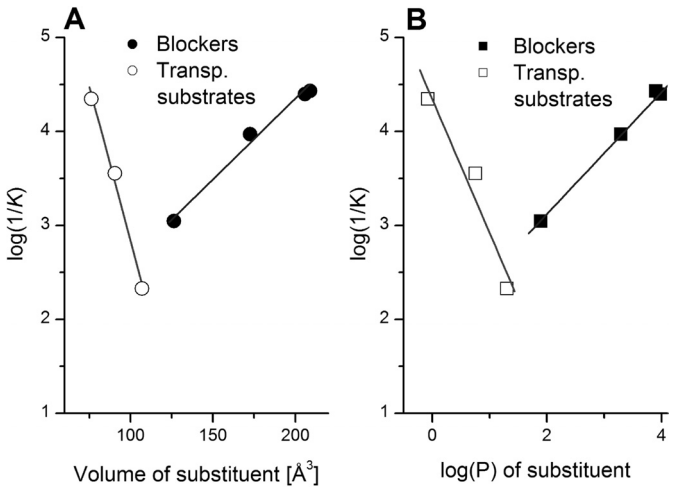

Fig. 7. Structure-activity relationships of ASCT2 ligands. Dependence of the apparent dissociation constant [log(1/K)] on the volume of the side-chain substituent (A) and the log(P) of the substituent (B). The substituent was defined as all side-chain atoms, starting from C_β, and excluding C_α and the α carboxy and amino groups. Substrates are shown as open symbols, and inhibitors are filled symbols. P, octanol-water partition coefficient.

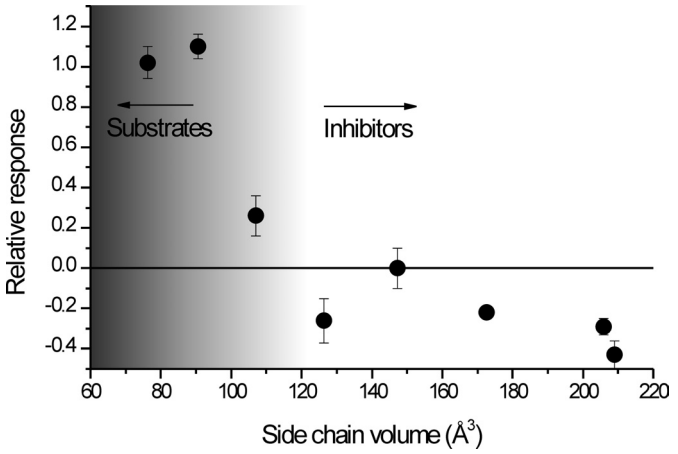

Fig. 8. Predicting substrate, partial substrate, or inhibitor behavior: the direction of the anion current scales with the side-chain volume. The anion current response was calculated relative to that induced by saturating alanine concentration (all at 0 mV).

that were chemically synthesized and tested with regard to their ability to activate or inhibit the ASCT2-mediated anion conductance, a measure for transport activity. The main new result from this study is that predictors, including side-chain hydrophobicity and volume, allow the classification of compounds into activating substrates, partial substrates, and inactivating inhibitors. The results will be useful to more accurately predict ligand behavior in the ASCT2 binding site.

Mechanism of Ligand Interaction with the Binding Site. For the related glutamate transporters, a model for ligand interaction emerges as follows: in the apo, ligand-free state, re-entrant loop 2 is in an open configuration, allowing low-affinity association of the transported substrate within the binding cleft. Binding is followed by closure of RL2, resulting in high-affinity interaction and allowing translocation across the membrane. Transported substrates presumably bind with higher affinity to the open-loop configuration, because the presence of RL2 allows for an increased number of hydrogen bonding contacts, as well as hydrophobic interactions between ligand and protein. Competitive inhibitors, such as TBOA, prevent loop closure by positioning the bulky benzyl moiety next to the open RL2, thus preventing translocation. Our docking studies are consistent with this model, suggesting that aspartate preferentially binds to the closed-loop conformation, thus stabilizing it, whereas TBOA preferentially binds to the open-loop configuration. Although a crystal structure of the apo configuration is not available, molecular dynamics studies point to the existence of an open-loop apo conformation (Huang and Tajkhorshid, 2008).

Our results for ligand binding to the highly homologous neutral amino acid transporter ASCT2 are consistent with these ideas. In particular, the docking results suggest that compounds that are transported by ASCT2 (activate the anion conductance) bind preferentially to the closed-loop configuration. In contrast, inhibitors are excluded from the closed-loop configuration because of steric clash, but they bind with significant docking scores to the open-loop configuration. Thus, it is likely that ASCT2 inhibitors prevent RL2 closure as a result of the steric inability of the inhibitor-ASCT2 complex to adopt a closed-loop configuration. Consistent with this model, inhibitor potency, in docking and in the experiment, scales with the volume, as well as the hydrophobicity of the amino acid side chain (Fig. 7). For transported substrates, our results suggest that they interact poorly with the open-loop configuration but strongly with the closed-loop configuration, thus shifting the equilibrium to the closed-loop form.

It should be noted that for the inhibitors with the more bulky aromatic substituents, such as fluorenyl and naphthyl, no poses were found, in which the aromatic group associates with the center of RL2. A plausible reason for this behavior is that the side chains are too bulky to fit into the TBOA-homologous open-loop configuration. This indicates that these inhibitors adopt a different side-chain conformation compared with benzylserine or TBOA, which have less aromatic bulk. Alternatively, RL2 may open even further upon substrate dissociation, generating additional room for side-chain interaction. This second alternative is supported by MD simulation results of Glt_{Ph}, in which the open-loop conformation on average showed a higher degree of RL2 opening than the TBOA-bound form (Huang and Tajkhorshid, 2008). Therefore, it can be speculated that RL2 can adopt varying degrees of opening, depending on the type of bound substrate, ranging from fully closed for the rapidly transported substrates, to partially closed for the partial substrates, to fully open for the bulkiest inhibitors. Such a mechanism would not be unprecedented, as in glutamate receptors, which rely on a Venus flytrap model for receptor activation by ligand binding (Abele et al., 1999; Armstrong and Gouaux, 2000), the efficacy of the ligand to induce channel opening depends on the degree of domain closure.

Our results suggest that the compound with the naphtyl substituent (**3c**) dissociates from its binding site with an apparent rate coefficient of $k_d = 72\ s^{-1}$. Assuming a dissociation constant of $K_d = 100\ \mu M$, an association rate constant of $k_b = 7 \times 10^5\ M^{-1}s^{-1}$ can be estimated (assuming that $K_d = k_d/k_b$). This rate constant is lower than expected for diffusion-controlled binding. Therefore, it can be hypothesized that binding of bulky inhibitors requires an additional conformational change of the ASCT2 binding site.

Predicting the Activating/Inhibiting Nature of the Substrate. One of the main objectives of this study was to be able to develop predictors of ASCT2 substrate behavior. Consistent with results for EAATs, hydrophobic bulk in the side chain aids high-affinity interaction with ASCT2, in particular if this bulk is aromatic. Side-chain volume can be used to discriminate between transported substrates and inhibitors (Fig. 8), with full substrates exhibiting side-chain volumes less than 100 $Å^3$. Inhibitors have side-chain volumes larger than 120 $Å^3$, with partial substrates somewhere in between. It is notable that there is a relatively sharp cutoff in side-chain volume between substrates and inhibitors.

It is noteworthy that it is not just hydrophobic bulk in the side chain that is necessary for high-affinity interaction, but this bulk needs to be aromatic. As shown in Table 2, compound **1c** with the cyclohexyl substituent did not interact with ASCT2. This indicates that a large, hydrophobic aliphatic group is not sufficient for binding, but that aromatic nature of the side chain is important. This requirement for aromatic nature is not well represented by the docking results, in which **3c** is predicted to bind to the open-loop form with a high docking score (Table 2). This is not surprising, because the scoring function includes only a general hydrophobic term in the absence of π-specific interactions (Trott and Olson, 2010). In the homology model, only two aromatic residues are in the vicinity of the binding site for potential π-stacking interaction (Phe391 and Trp459), but both of these side chains are too far away from the predicted binding location of the aromatic ring(s). Therefore, the detailed physical description of the binding site interaction awaits further study.

ASCT2 Pharmacology. Relatively few inhibitors for amino acid transport by ASCT2 have been developed. In one study, benzylserine was found to be a prototypic competitive ASCT2 inhibitor, based on its structural similarity to the glutamate transporter blocker TBOA (Grewer and Grabsch, 2004). However, benzylserine binds with somewhat low affinity (~1 mM). In another report, a series of asparagine derivatives was investigated, with aromatic groups linked to the amide nitrogen (Esslinger et al., 2005). Although no K_i values were given for the compounds, the most potent inhibitor, *p*-nitrophenyl glutamyl anilide, inhibited 50% of the uptake at approximately 0.25 mM (Esslinger et al., 2005). Although not knowing the exact K_m value of the C6-cell glutamine transporter for glutamine, it can be estimated that the actual K_i of the compound is approximately 80 μM at 100 μM glutamine. Our most potent inhibitor based on the biphenyl moiety binds with a 30 μM apparent affinity (Table 2), suggesting that this represents the highest affinity inhibitor for ASCT2 known to date, surpassing the previous compound in potency by at least a factor of 3.

It is noteworthy that the study by Esslinger et al. (2005) concluded that a H-bond donor in the side chain, in the form of the amide N-H group, is important for high-affinity interaction. However, in our series of compounds no hydrogen bond donor is present at this position. This result suggests that the H-bond donor is not required for high-affinity interaction of inhibitors with the ASCT2 binding site, but it does not exclude the possibility that the introduction of a H-bond donor to the fluorenyl compound could increase affinity. This possibility may be tested in future experiments.

A significant problem for the development of ASCT2 inhibitors is specificity. For example, aryl-asparagine derivatives have been reported as high-affinity inhibitors for glutamate transporters (Greenfield et al., 2005). This indicates that the absence of the negatively charged β-carboxylate group does not abolish interaction with the binding site of EAATs. The ASCT2 inhibitors tested here, except benzylserine, also consistently inhibit the glutamate transporter EAAT3 (data not shown). This is an important finding; it means that cell biological or neurophysiological studies relying on pharmacological inhibition of glutamate transporters have to be evaluated carefully, because many of the known EAAT inhibitors may also inhibit ASCTs, although their ASCT2 action has never been tested. Therefore, effects may be ascribed to inhibition of EAATs that may partially be caused by inhibition of neutral amino acid transporters. Therefore, it remains a challenge to develop high-affinity inhibitors that preferentially bind to ASCTs over EAATs. Pure reliance on hydrophobic bulk in the side chain to achieve high-affinity interaction will not be sufficient to generate selectivity. Specificity may also be difficult to achieve with respect to other neutral amino acid transporter families. The pharmacology of the system A and system N transporters is not well established, preventing us from commenting on a possible interaction of our compounds with these transporters. For the system L amino acid transporters, LAT, amino acids with aromatic side chains are substrates (Segawa et al., 1999). Therefore, it is conceivable to assume that aromatic serine esters may also interact with the LAT family of amino acid transporters.

Conclusions

In summary, we have used a docking approach, together with experimental validation, to predict substrate and inhibitor behavior of a series of serine derivatives that interact with the binding site of the neutral amino acid transporter ASCT2. Our model predicts that amino acid derivatives with small side-chain volume and low side-chain hydrophobicity interact strongly with the closed-loop form of the binding site but bind weakly to the open-loop form, acting as transported substrates. In contrast, inhibitors bind preferentially to the open-loop form. Side-chain aromaticity is required for high-affinity interaction. These predictions allowed us to develop an inhibitor that binds to ASCT2 with 30 μM apparent affinity, which to our knowledge is currently unsurpassed by other ASCT2 inhibitors. In light of the presumed importance of ASCT2 in glutamine release from proliferating astrocytes, thus potentially contributing to the glutamate-glutamine cycle (Bröer and Brookes, 2001), as well as the well known up-regulation of ASCT2 in many cancers (Fuchs and Bode, 2005), the development of new ASCT2 inhibitors may lead to compounds of therapeutic value.

Authorship Contributions

Participated in research design: Albers and Grewer.

Conducted experiments: Albers, Marsiglia, Gameiro, and Grewer.

Contributed new reagents or analytic tools: Albers, Marsiglia, and Thomas.

Performed data analysis: Albers, Marsiglia, Gameiro, and Grewer.

Wrote or contributed to the writing of the manuscript: Albers, Marsiglia, Gameiro, and Grewer.

References

Abele R, Svergun D, Keinänen K, Koch MH, and Madden DR (1999) A molecular envelope of the ligand-binding domain of a glutamate receptor in the presence and absence of agonist. *Biochemistry* **38:**10949–10957.

Armstrong N and Gouaux E (2000) Mechanisms for activation and antagonism of an AMPA-sensitive glutamate receptor: crystal structures of the GluR2 ligand binding core. *Neuron* **28:**165–181.

Arriza JL, Kavanaugh MP, Fairman WA, Wu YN, Murdoch GH, North RA, and Amara SG (1993) Cloning and expression of a human neutral amino acid transporter with structural similarity to the glutamate transporter gene family. *J Biol Chem* **268:**15329–15332.

Bass R, Hedegaard HB, Dillehay L, Moffett J, and Englesberg E (1981) The A, ASC, and L systems for the transport of amino acids in Chinese hamster ovary cells (CHO-K1). *J Biol Chem* **256:**10259–10266.

Bendahan A, Armon A, Madani N, Kavanaugh MP, and Kanner BI (2000) Arginine 447 plays a pivotal role in substrate interactions in a neuronal glutamate transporter. *J Biol Chem* **275:**37436–37442.

Bode BP (2001) Recent molecular advances in mammalian glutamine transport. *J Nutr* **131:**2475S–2485S.

Boudker O, Ryan RM, Yernool D, Shimamoto K, and Gouaux E (2007) Coupling substrate and ion binding to extracellular gate of a sodium-dependent aspartate transporter. *Nature* **445:**387–393.

Bridges RJ and Esslinger CS (2005) The excitatory amino acid transporters: pharmacological insights on substrate and inhibitor specificity of the EAAT subtypes. *Pharmacol Ther* **107:**271–285.

Bridges RJ, Kavanaugh MP, and Chamberlin AR (1999) A pharmacological review of competitive inhibitors and substrates of high-affinity, sodium-dependent glutamate transport in the central nervous system. *Curr Pharm Des* **5:**363–379.

Bröer A, Brookes N, Ganapathy V, Dimmer KS, Wagner CA, Lang F, and Bröer S (1999) The astroglial ASCT2 amino acid transporter as a mediator of glutamine efflux. *J Neurochem* **73:**2184–2194.

Bröer A, Wagner C, Lang F, and Bröer S (2000) Neutral amino acid transporter ASCT2 displays substrate-induced Na+ exchange and a substrate-gated anion conductance. *Biochem J* **346:**705–710.

Bröer S and Brookes N (2001) Transfer of glutamine between astrocytes and neurons. *J Neurochem* **77:**705–719.

Deitmer JW, Bröer A, and Bröer S (2003) Glutamine efflux from astrocytes is mediated by multiple pathways. *J Neurochem* **87:**127–135.

Dunlop J and Butera JA (2006) Ligands targeting the excitatory amino acid transporters (EAATs). *Curr Top Med Chem* **6:**1897–1906.

Dunlop J, Eliasof S, Stack G, McIlvain HB, Greenfield A, Kowal D, Petroski R, and Carrick T (2003) WAY-855 (3-amino-tricyclo[2.2.1.02.6]heptane-1,3-dicarboxylic acid): a novel, EAAT2-preferring, nonsubstrate inhibitor of high-affinity glutamate uptake. *Br J Pharmacol* **140:**839–846.

Esslinger CS, Cybulski KA, and Rhoderick JF (2005) Ngamma-aryl glutamine analogues as probes of the ASCT2 neutral amino acid transporter binding site. *Bioorg Med Chem* **13:**1111–1118.

Eswar N, Webb B, Marti-Renom MA, Madhusudhan MS, Eramian D, Shen MY, Pieper U and Sali A (2007) Comparative protein structure modeling using MODELLER. *Curr Protoc Protein Sci* **Chapter** 2:Unit 2 9.

Fuchs BC and Bode BP (2005) Amino acid transporters ASCT2 and LAT1 in cancer: partners in crime? *Semin Cancer Biol* **15:**254–266.

Gliddon CM, Shao Z, LeMaistre JL, and Anderson CM (2009) Cellular distribution of the neutral amino acid transporter subtype ASCT2 in mouse brain. *J Neurochem* **108:**372–383.

Greenfield A, Grosanu C, Dunlop J, McIlvain B, Carrick T, Jow B, Lu Q, Kowal D, Williams J, and Butera J (2005) Synthesis and biological activities of aryl-ether-, biaryl-, and fluorene-aspartic acid and diaminopropionic acid analogs as potent inhibitors of the high-affinity glutamate transporter EAAT-2. *Bioorg Med Chem Lett* **15:**4985–4988.

Grewer C, Balani P, Weidenfeller C, Bartusel T, Tao Z, and Rauen T (2005) Individual subunits of the glutamate transporter EAAC1 homotrimer function independently of each other. *Biochemistry* **44:**11913–11923.

Grewer C and Grabsch E (2004) New inhibitors for the neutral amino acid transporter ASCT2 reveal its Na^+-dependent anion leak. *J Physiol* **557:**747–759.

Grewer C, Watzke N, Wiessner M, and Rauen T (2000) Glutamate translocation of the neuronal glutamate transporter EAAC1 occurs within milliseconds. *Proc Natl Acad Sci USA* **97:**9706–9711.

Hamill OP, Marty A, Neher E, Sakmann B, and Sigworth FJ (1981) Improved patch-clamp techniques for high-resolution current recording from cells and cell-free membrane patches. *Pflugers Arch* **391:**85–100.

Huang Z and Tajkhorshid E (2008) Dynamics of the extracellular gate and ion-substrate coupling in the glutamate transporter. *Biophys J* **95:**2292–2300.

Luethi E, Nguyen KT, Bürzle M, Blum LC, Suzuki Y, Hediger M, and Reymond JL (2010) Identification of selective norbornane-type aspartate analogue inhibitors of the glutamate transporter 1 (GLT-1) from the chemical universe generated database (GDB). *J Med Chem* **53:**7236–7250.

Neu J, Shenoy V, and Chakrabarti R (1996) Glutamine nutrition and metabolism: where do we go from here ? *FASEB J* **10:**829–837.

Segawa H, Fukasawa Y, Miyamoto K, Takeda E, Endou H, and Kanai Y (1999) Identification and functional characterization of a Na^+-independent neutral amino acid transporter with broad substrate selectivity. *J Biol Chem* **274:**19745–19751.

Sheehan JC, Goodman M, and Hess GP (1956) Peptide derivatives containing hydroxyamino acids. *J Am Chem Soc* **78:**1367–1369.

Shimamoto K, Lebrun B, Yasuda-Kamatani Y, Sakaitani M, Shigeri Y, Yumoto N, and Nakajima T (1998) DL-*threo*-β-Benzyloxyaspartate, a potent blocker of excitatory amino acid transporters. *Mol Pharmacol* **53:**195–201.

Söding J, Biegert A, and Lupas AN (2005) The HHpred interactive server for protein homology detection and structure prediction. *Nucleic Acids Res* **33:**W244–W248.

Trott O and Olson AJ (2010) AutoDock Vina: improving the speed and accuracy of docking with a new scoring function, efficient optimization, and multithreading. *J Comput Chem* **31:**455–461.

Utsunomiya-Tate N, Endou H, and Kanai Y (1996) Cloning and functional characterization of a system ASC-like Na^+-dependent neutral amino acid transporter. *J Biol Chem* **271:**14883–14890.

Wallner B and Elofsson A (2003) Can correct protein models be identified? *Protein Sci* **12:**1073–1086.

Watzke N, Bamberg E, and Grewer C (2001) Early intermediates in the transport cycle of the neuronal excitatory amino acid carrier EAAC1. *J Gen Physiol* **117:**547–562.

Watzke N and Grewer C (2001) The anion conductance of the glutamate transporter EAAC1 depends on the direction of glutamate transport. *FEBS Lett* **503:**121–125.

Wolf LK (2009) New software and websites for the chemical enterprise. *Chem Engineering News* **87:**31.

Yernool D, Boudker O, Jin Y, and Gouaux E (2004) Structure of a glutamate transporter homologue from *Pyrococcus horikoshii*. *Nature* **431:**811–818.

Zerangue N and Kavanaugh MP (1996) ASCT-1 is a neutral amino acid exchanger with chloride channel activity. *J Biol Chem* **271:**27991–27994.

Address correspondence to: Dr. Christof Grewer, Department of Chemistry, Binghamton University, 4400 Vestal Parkway East, Binghamton, NY 13902. E-mail: cgrewer@binghamton.edu